IEEE Photonics Journal
An IEEE Photonics Society Publication

Open Access

Sampling Time Adaptive Single-Photon Compressive Imaging

Volume 11, Number 3, June 2019

Hui Wang
Qiurong Yan
Bing Li
Chenglong Yuan
Yuhao Wang

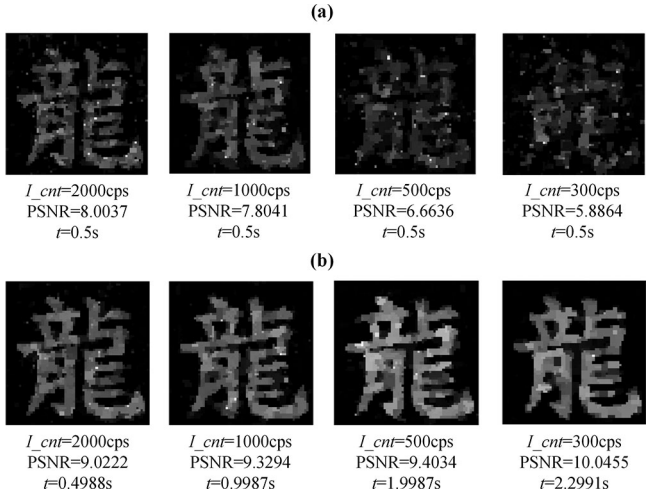

DOI: 10.1109/JPHOT.2019.2912326
1943-0655

Sampling Time Adaptive Single-Photon Compressive Imaging

Hui Wang,[1] Qiurong Yan ,[1,2] Bing Li,[1] Chenglong Yuan,[1] and Yuhao Wang [1]

[1]Department of Electronics Information Engineering, Nanchang University, Nanchang 330031, China
[2]State Key Laboratory of Transient Optics and Photonics, Xi'an Institute of Optics and Precision Mechanics, Chinese Academy of Sciences, Xi'an 710119, China

DOI:10.1109/JPHOT.2019.2912326

Manuscript received March 12, 2019; revised April 11, 2019; accepted April 15, 2019. Date of publication May 1, 2019; date of current version May 13, 2019. This work was supported in part by the National Natural Science Foundation of China under Grant 61865010 and Grant 61565012, in part by the China Postdoctoral Science Foundation under Grant 2015T80691, in part by the Science and Technology Plan Project of Jiangxi Province under Grant 20151BBE50092, and in part by the Funding Scheme to Outstanding Young Talents of Jiangxi Province under Grant 20171BCB23007. Corresponding author: Qiurong Yan (e-mail: yanqiurong@ncu.edu.cn).

Abstract: We propose a time-adaptive sampling method and demonstrate a sampling-time-adaptive single-photon compressive imaging system. In order to achieve self-adapting adjustment of sampling time, the theory of threshold of light intensity estimation accuracy is deduced. According to this threshold, a sampling control module, based on field-programmable gate array, is developed. Finally, the advantage of the time-adaptive sampling method is proved experimentally. Imaging performance experiments show that the time-adaptive sampling method can automatically adjust the sampling time for the change of light intensity of image object to obtain an image with better quality and avoid speculative selection of sampling time.

Index Terms: Time-adaptive sampling, single photon compressive imaging, threshold of light intensity estimation accuracy.

1. Introduction

Single photon compressive imaging is a very efficient implementation of compressed sensing (CS) theory in photon counting imaging. In this imaging method, a digital micro-mirror device (DMD) is used to modulate the optical image of target and a single photon point detector is used to detect the modulated light. The photon counts output by the detector and the random binary patterns loaded into DMD are used to reconstruct the target image by CS reconstruction algorithm [1]–[7]. Owing to the use of CS theory, single photon compressive imaging can perform compressive sampling of images, which not only shortens the sampling time and saves the storage space, but also improves signal-to-noise ratio (SNR) [8]. Therefore, it has broad application prospects in ultra-weak light imaging detection, such as medical diagnosis, astronomical observation, spectral measurement [9]–[14], etc.

In the single photon compressive imaging system reported in the literature, the DMD is set to a fixed flip or modulation frequency, which means that each sampling time is of equal length [7], [8], [15]–[18]. And then the numbers of detected photon in the equal time intervals are used

as the measured values to restore the original image. Wen-Kai Yu *et al.* utilized this sampling method to achieve single photon compressive imaging with a sampling frequency of 34 Hz [7]; Howland *et al.* also used this sampling method to achieve photon counting compressive depth image reconstruction with a speed of 14 frame per second, and then used it for real-time tracking of 3D objects [19]–[22].

As we know, when photon counting technology is used to measure light intensity, prolonging the sampling time can suppress the influence of Poisson noise, thereby increasing the SNR. Since the light intensity reflected by the DMD is different at each measurement in the single-photon compressive imaging system, the SNR of each measurement is different due to different photon counts in the equal time intervals. When the imaging target is very weak, if the DMD flips too fast, the SNR of some measurements is too low, causing the reconstructed image to deteriorate or even fail to reconstruct. Of course, if the DMD flips too slowly, it will consume too much unnecessary time for imaging, ultimately affecting the real-time performance of the imaging system. So constantly tried methods are used to determine an appropriate flip frequency to balance imaging quality and sampling time.

More and more scholars have conducted researches on adaptive compressive imaging in recent years [22]–[33]. S. Dekel first proposed to obtain low-resolution image from the previous sampling, and then sample the important region based on the wavelet or dictionaries coefficients of low-resolution image, and finally performed the inverse wavelet transform to reconstruct the high-resolution image [27], [28]. Aßmann and Bayer proposed a compressive adaptive computational ghost imaging method [29]. Dai introduced an adaptive compressed sampling method based on extended wavelet trees [30]. Wen-Kai Yu *et al.* proposed the regions corresponding to important wavelet coefficients can be regards as a whole and imaged by applying CS instead of point scanning [31]. F. Rousset predicted important wavelet coefficients based on fast cubic interpolation in the image domain and quantized them to use any kind of wavelet [32]. Rousset *et al.* proposed the time-resolved adaptive multispectral imaging method based on single-pixel camera, which used an adaptive acquisition strategy called “Wavelet Predictive Adaptive Datum Scanning” to improve the resolution and shorten the imaging time [33]. The above adaptive methods first collect low-resolution images, obtain prior information, and then adjust the random matrix loaded into the DMD to obtain high-resolution images and thereby reduce the total acquisition time. Moreover, recently, the first photon imaging technique was first proposed in scanning imaging [34]. The laser pulse is continuously emitted to the pixel unit at the scanning position until the first reflected photon is detected, and then the next scanning position is performed. The intensity of the light at the scanning point is estimated by recording the number of laser pulses that have been emitted, so the sampling time per pixel is not fixed. Techniques for measuring light intensity using the first photon are proposed for ghost imaging [35]. The reflected light intensity of DMD is measured by detecting the first photon. The image can be reconstructed from less than 0.1 detected photon per pixel [36]. Since the DMD reflected light intensity is different at each sampling, the dwell time of DMD is not fixed.

In this paper, we proposed a time-adaptive sampling method for single photon compressive imaging system. The time of each measurement is not the same, and it is automatically adjusted according to the DMD reflected light intensity. The performance of the time-adaptive sampling method is verified by experiments.

2. Large-Area Single Photon Imaging With Compressive Sensing

2.1 Imaging Principle

A diagram of the experimental apparatus is shown in Fig. 1. The light source, which is collimated into parallel light by a collimator, emits extremely weak parallel light. The object is illuminated by the parallel light and then imaged onto the DMD via an imaging lens. The DMD consists of 1024×768 micromirrors with size $13.68\ \mu\text{m} \times 13.68\ \mu\text{m}$. Each mirror can be individually controlled to deflect ± 12 degrees. The rotating angles of micromirrors can be controlled synchronously by a binary

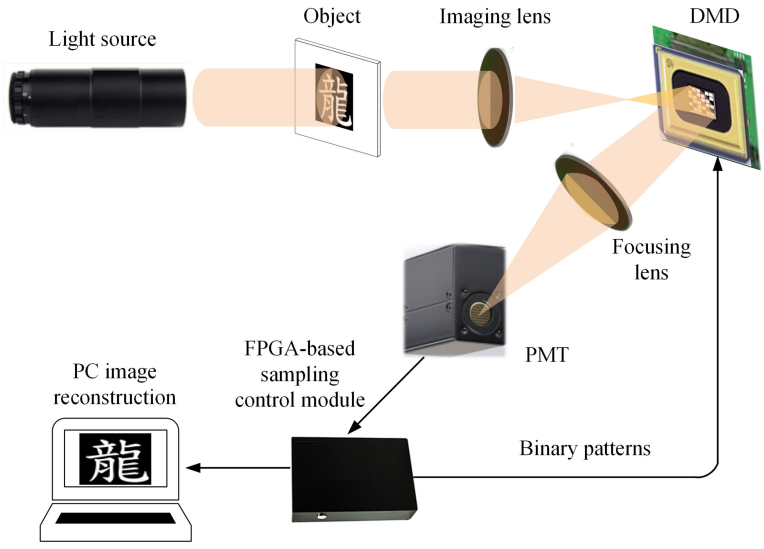

Fig. 1. Experimental apparatus for single photon compressive imaging. DMD: digital micromirror device, PMT: photomultiplier tube, FPGA: field programmable gate array, PC: personal computer.

random pattern loaded into the DMD. The micromirrors corresponding to the element "1" in the matrix deflect $+12$ degrees, and the micromirrors corresponding to the element "0" in the matrix deflect -12 degrees. A focusing lens is set along the $+12$ degrees direction of DMD to collect reflected light into a single photon detector. In order to perform M compressive samplings on the optical image, the sampling control module sequentially loads M random binary patterns into the DMD, and synchronously records the light intensity information received by the detector each sampling. Then the image can be recovered by CS algorithm according to the measurement matrix A and the light intensity I.

In the imaging method of the existing literatures, the total sampling time is fixed and M samplings are equal time interval samplings. That is to say, assuming that the preset total sampling time is T_{tot}, the time of each sampling can be calculated as $t = T_{tot}/M$. For each sampling, a random pattern is loaded into the DMD controlled by the sampling control module. During each sampling interval t, the number of detected photons n is recorded synchronously. These numbers of detected photons in equal time interval, which are considered to be the characterization of the modulated light intensity, are input into the CS algorithm for image restoration.

However, for uncertain imaging targets, the above time-fixed sampling method perform poor robustness. Too short sampling time will lead to some samplings with very low SNRs, so that the signal will be obliterated in the noise. And too long sampling time will lead to sampling saturation. Therefore, it is difficult to set the optimal sampling time to balance sampling time and imaging quality under different light levels. Based on this, a time-adaptive sampling method is proposed in this paper. In our sampling method, firstly the intensity of modulated light is no longer represented by the number of photons detected in equal time intervals, but estimated by the arrival time intervals of photons detected continuously. Secondly, the time of each sampling t is no longer fixed, while the estimation accuracy of light intensity of each sampling is controlled to reach a threshold. That is, only when the estimation accuracy of light intensity of one sampling reaches this threshold, one sampling is considered complete, and therefore the sampling time can be adapted to different light intensity levels. Thirdly, the number of detected photons P_i in each sampling and the time of each sampling t_i are recorded synchronously. The ratio of P_i to t_i can be used as the measured values for image reconstruction. In this method, only the sampling time is adjusted adaptively, and DMD patterns and reconstruction algorithm involved in the experiment need not be specially designed.

2.2 Threshold of Light Intensity Estimation Accuracy

In our time-adaptive sampling method, as mentioned earlier, the arrival time intervals of photons are measured, and then the modulated light intensity is estimated by the photon arrival time intervals. Here, to determine the threshold of estimation accuracy, we use the maximum likelihood method to estimate the light intensity based on the data of photon arrival time interval.

Assuming that the arrival time intervals of n continuously detected photons are $t_1, t_2, t_3, \ldots, t_n$ respectively, the photon counting rate under this light intensity condition is λ cps. Then the random vector $t = [t_1\ t_2 \ldots\ t_n]$ can be regarded as a set of observations of the event population $\mathbf{T} = [T_1\ T_2 \ldots\ T_n]$. Since the photon emission process is a Poisson process, assuming that its emission rate is λ, the probability of $N(t)$ photons being emitted within a time interval t is:

$$P\{N(t) = n\} = e^{-\lambda t}\frac{(\lambda t)^n}{n!},\ n = 0, 1, \ldots, \tag{1}$$

Let T_1 denote the emitted time of the first photon of the Poisson process, then the probability distribution function of the emission time of the first photon is:

$$P\{T_1 \le t\} = 1 - P\{T_1 > t\} = 1 - e^{-\lambda t} \tag{2}$$

For $n \ge 2$, let T_n denote the emitted time interval between the nth photon and the $(n-1)$st photon. Then the probability distribution function of T_n is:

$$\begin{aligned} P\{T_n \le t\} &= 1 - P\{T_n > t\} \\ &= 1 - P\{N((T_{n-1} + t) - T_{n-1}) = 0\} \\ &= 1 - e^{-\lambda t} \end{aligned} \tag{3}$$

Taking the derivative of the above Eq. (2) and (3), the probability density function of the adjacent photons emission time interval can be expressed as [37]:

$$p(t) = \lambda e^{-\lambda t} \tag{4}$$

Since the photon detection process is also a Poisson process, the probability density function of the adjacent photon arrival time interval at the detector can also be expressed by Eq. (4). Therefore, for a light intensity stable condition with a photon counting rate of λ, the conditional probability density function of the photon arrival time interval can be written as:

$$p(t/\lambda) = \lambda e^{-\lambda t}\,(t > 0) \tag{5}$$

So, the likelihood function of the observation vector $\mathbf{t}$ is:

$$\begin{aligned} L(\mathbf{t};\lambda) &= \prod_{i=1}^{n} p(t_i/\lambda) \\ &= \lambda^n e^{-\left(\sum_{i=1}^{n} t_i\right)\lambda} \end{aligned} \tag{6}$$

Since $\ln L(\mathbf{t};\lambda)$ and $L(\mathbf{t};\lambda)$ have the same monotonicity, the maximum likelihood estimator of the parameter λ can be obtained from the likelihood equation shown in Eq. (7).

$$\frac{\partial \ln L(\mathbf{t};\lambda)}{\partial \lambda} = \frac{n}{\lambda} - \sum_{i=1}^{n} t_i = 0 \tag{7}$$

According to Eq. (7), the maximum likelihood estimator of λ is:

$$\lambda = \frac{n}{t_1 + t_2 + t_3 + \ldots t_n} \tag{8}$$

According to the statistical knowledge of the exponential distribution, the mean and variance of t are $1/\lambda$ and $1/\lambda^2$ respectively. Take the estimated error as the ratio of the standard deviation to the mean. Note that the standard deviation and the mean in refer to the standard deviation of

the sample mean and the mean of the sample mean, i.e., the standard deviation and the mean of the population **T**. This is because that the estimation error depends on the estimation results of a large number of samples, rather than the estimation results of a certain sample. Moreover, the relationship between the mean and variance of the population and the mean and variance of the sample is as follows:

$$\begin{cases} E\left(\bar{T}\right) = E\left(\bar{t}\right) = 1/\lambda \\ D\left(\bar{T}\right) = \frac{1}{n} D\left(\bar{t}\right) = \frac{1}{n\lambda^2} \end{cases} \tag{9}$$

Where $E(\bar{T})$ and $D(\bar{T})$ are the mean and the variance of the population **T** respectively, and $E(\bar{t})$ and $D(\bar{t})$ are the mean and the variance of the sample t respectively. So, the estimated error can be expressed as:

$$\Delta = \sqrt{\frac{D\left(\bar{T}\right)}{\left[E\left(\bar{T}\right)\right]^2}} = \sqrt{\frac{1/n\lambda^2}{1/\lambda^2}} = \frac{1}{\sqrt{n}} \tag{10}$$

From Eq. (10), it can be seen that the time-adaptive sampling with equal estimation accuracy can be achieved by controlling the photon number of each sampling to a certain value. In this way, not only time-adaptive sampling is realized, but also the estimation accuracy of modulated light intensity of each sampling is equal, which is advantageous for compressed sensing image reconstruction. Since controlling the light intensity estimation accuracy to a certain threshold is equivalent to controlling the light intensity estimation error below a certain value, a specific estimation error is taken as the threshold, and when the estimated error is lower than the threshold, one sampling is controlled to end.

2.3 Implementation of Control Circuit

As analyzed above, setting the estimation accuracy of a single sampling is equivalent to setting the number of photons detected in a single sampling. Therefore, in the actual experiment, the equal estimation accuracy samplings are achieved by controlling the number of photons per sampling to a fixed value $P_i = \mathrm{P}$.

In order to realize this equal estimation accuracy samplings, a FPGA-based sampling control module is designed. The timing diagram of M samplings is shown in Fig. 2. 1) When the rising edge of the start sampling signal is received, the counter that counts sampling number is incremented by one, and the sampling control module outputs the first sampling control pulse to control the DMD to perform one modulation of the original image; 2) when the rising edge of the sampling control pulse signal is received, photon counter and pulse interval counter start to count single photon pulses and high frequency clock pulses respectively; 3) when the photon counter counts to the present value P, the sampling control module outputs the value in the pulse interval counter to the PC and then clears the photon counter and pulse interval counter. If the value in sampling number counter is small than $M + 1$, the next sampling control pulse is output, and the sampling number counter is incremented by one; 4) repeat steps 2)-3) until that the sampling number counter counts to $M + 1$, and then stop sampling. All values output from pulse interval counter are used as the time of each sampling for image reconstruction. In this paper, this sampling control module is implemented on Altera Cyclone IV FPGA and the time bin resolution is 20 ns.

3. Experimental Results and Discussion

3.1 Time-Adaptive Sampling Verification

To verify the sampling time adaptive advantage of our proposed method, a group of imaging experiments under different light levels are completed. For accurate evaluation of image reconstruction quality, the full reference evaluation index Peak Signal to Noise Ratio (PSNR) is used to evaluate reconstructed images. In order to obtained the original image easily, in the experiment, instead

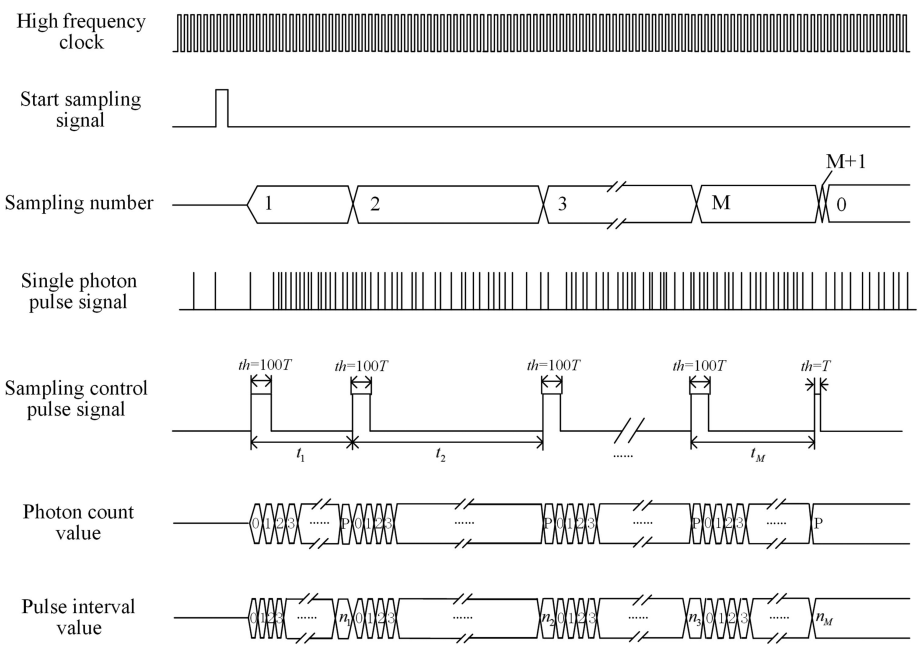

Fig. 2. Timing diagram of FPGA-based sampling control module. th: The high-level duration of one period of the sampling control signal. T: A period of the high frequency clock signal.

of placing the real object in the light path, we make that random patterns loaded into DMD are multiplied by the original image matrix frame by frame. Moreover, due to good edge recovery advantages, the TVAL3 (Total variation Augmented Lagrangian Alternating Direction Algorithm) is used to reconstruct images in this paper [38]–[40]. Firstly, as a comparison, the imaging results of the fixed time sampling method with different light levels are shown in Fig. 3(a). The time of each sampling is set to 0.5 s. Here, four different light levels are obtained by adjusting the voltage of light source. And the light intensity is characterized by the photon counting rate detected by PMT, which is about 2000 counts/s, 1000 counts/s, 500 counts/s and 300 counts/s respectively. And the imaging results of our time-adaptive sampling method under the same conditions are given in Fig. 3(b). The imaging resolutions are all 64 $\times$ 64. And the fixed photon number of each sampling for the sampling time adaptive imaging method is 1000. For intuitive observation of time adaptive effect, the average time of each sampling is also given in the figure.

From Fig. 3, it can be seen that, since the sampling time of the time-fixed imaging method is preset, when the light intensity is strong, this method can achieve the reconstruction of the target image, but when the light intensity is gradually weakened, the imaging result of the fixed sampling time method cannot be resolved. Usually, it is necessary to constantly try to find the right sampling time so that the reconstructed image can be displayed clearly. However, as the light intensity changes, the sampling time adaptive imaging method can automatically adjust the sampling time to obtain better image reconstruction quality. Therefore, the sampling time adaptive single photon compressive imaging can achieve compressive sampling and reconstruction in an adaptive manner under different light levels.

3.2 Time-Adaptive Imaging Performance

The time-adaptive sampling under different light levels can be achieved by our proposed method. However, both the imaging performance of this method and the influence of threshold setting on imaging effects need to be further analyzed. As a comparison, a threshold setting method, called light intensity related threshold, is introduced. In this method, the threshold setting no longer only

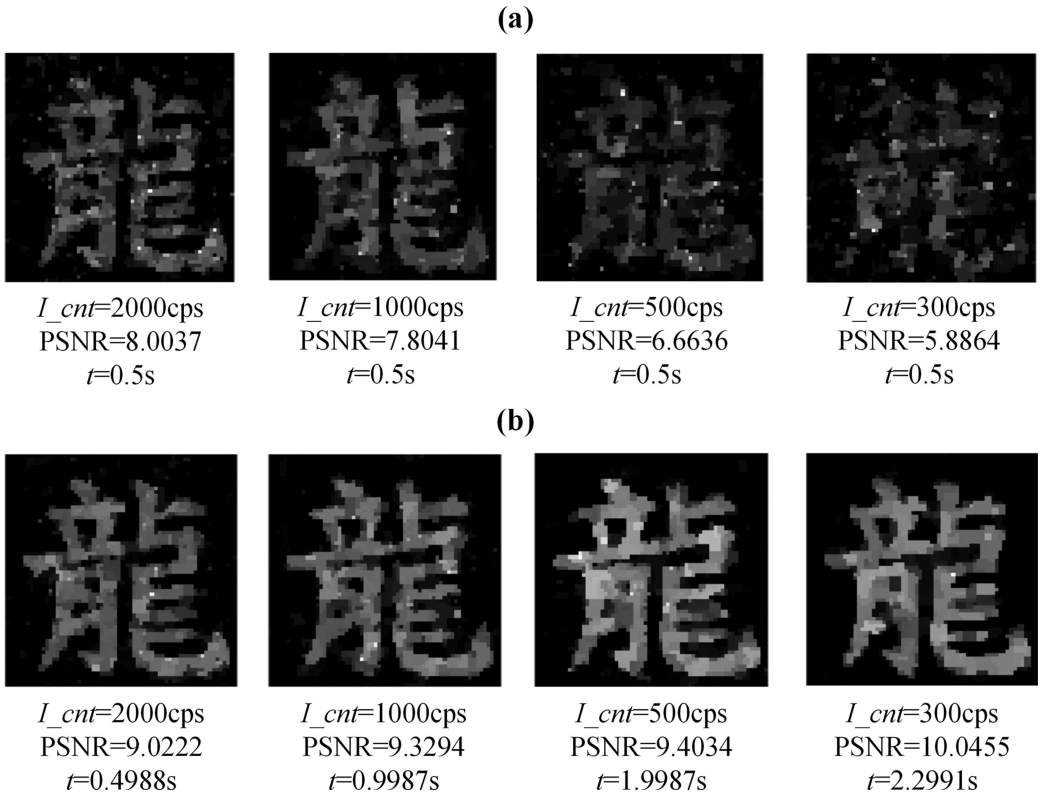

Fig. 3. Imaging results of two imaging methods with different light levels. (a) The imaging results of the fixed time sampling method with different light levels, the time for each sampling is set to 0.5 s. (b) The imaging results of the time-adaptive sampling method with different light levels, the fixed photon number of each sampling is 1000.

considers the estimation error, but is based on the product of the modulation light intensity and the estimation error. It can be expressed as:

$$I \cdot \frac{1}{\sqrt{n}} \geq \delta \tag{11}$$

Where δ refers to a custom constant threshold. And the corresponding FPGA-based control circuit realizes single sampling control by the following formula.

$$n \geq \delta^2 (t_1 + t_2 + \cdots + t_n)^2 \tag{12}$$

Where n is the number of photons in a single sampling and t_n is the arrival time interval of adjacent photons.

Then, to evaluate the performance of our time-adaptive imaging method, three methods above, the existing time-fixed imaging, our time-adaptive imaging and the imaging corresponding to the light intensity related threshold, are used for the compressive sampling and reconstruction experiments respectively with different average time of each sampling. And in each group of comparative experiments, the total sampling time of the three methods is controlled to be the same. The time control method is as follows. Firstly, the fixed photon number of each sampling n of the time-adaptive imaging is set, and then the total sampling time is counted after 2500 samplings. Then this time is set as the total sampling time of the time-fixed imaging. Finally, the total sampling time of the third method is made equal to the time above by adjusting δ. The experimental results are shown in Fig. 4. Some of reconstructed images are shown in Fig. 4(a). In addition, for an intuitive comparison, the Peak Signal to Noise Ratio (PSNR) of reconstructed images versus the average time

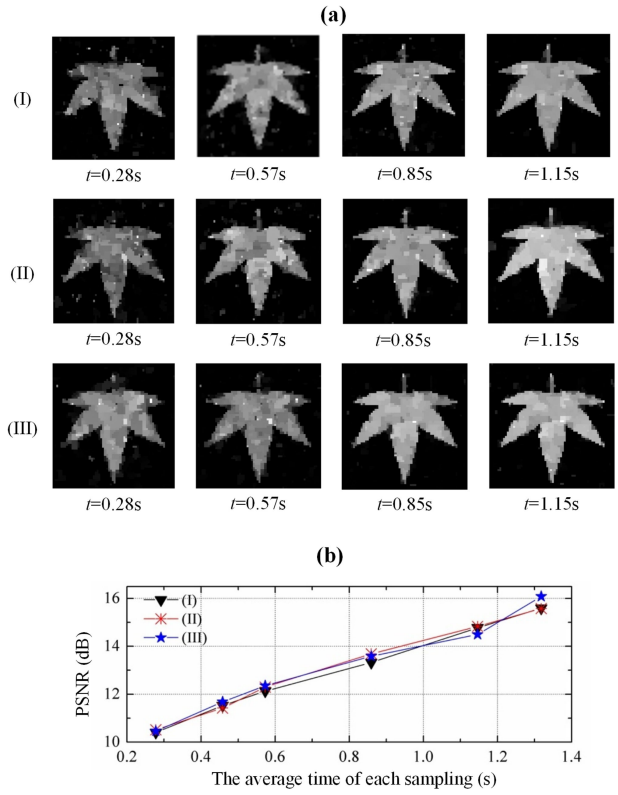

Fig. 4. Experimental results of three imaging methods, the existing time-fixed imaging (I), our time-adaptive imaging (II) and the imaging corresponding to the light intensity related threshold (III). (a) Some of reconstructed images. (b) The PSNRs of reconstructed images versus the average time of each sampling. Each data point takes the average of 100 independent experimental results.

of each sampling is given in Fig. 4(b). And each data point takes the average of 100 independent experimental results. The imaging resolution is 64 $\times$ 64.

From Fig. 4(a), we can see that image reconstruction performance of all three methods is enhanced with the increase of average time of each sampling. However, when the average time of each sampling is the same, the quality of images reconstructed by the three methods is almost the same. This conclusion can also be drawn from Fig. 4(b). Therefore, the time-adaptive imaging proposed in this paper does not degrade imaging performance while implementing time-adaptive sampling.

Compared to the time-fixed imaging, the error of light intensity estimation in our time-adaptive imaging is the same every time. But why does our method not obtain better imaging performance? And why does the threshold setting method have no obvious influence on imaging performance? As analyzed in Section 2.2, the number of photons in each sampling can be used as a characterization of the accuracy of light intensity estimation. So statistics on the numbers of photon in 2500 samplings of one group of experiments are made. The statistical results are shown in Fig. 5. In this group of experiments, the fixed number of each sampling of the time-adaptive imaging is 1000, and the total sampling time of three imaging methods is controlled to be the same.

From Fig. 5, it can be seen that, the concentration degree of photon number distribution: II $>$I$>$III. Compared to our fixed photon number threshold, other threshold setting methods will make the photon number distribution more dispersed. In theory, the more concentrated the photon number distribution, the uniformity of the light intensity estimation accuracy of each sampling, and the smaller the influence of the estimation error on the reconstruction result. However, in the usual experiment, the number of photons is on the order of 10^3, so the corresponding estimated error is

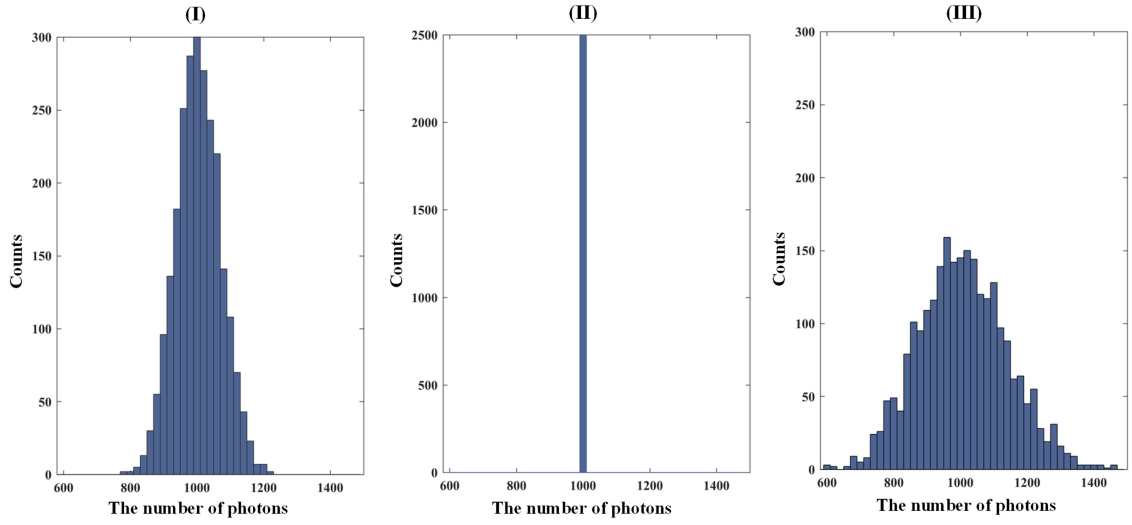

Fig. 5. Statistical results of the numbers of single-sampled photons with two methods. (I) The results of the fixed time sampling method. (II) The results of the time-adaptive imaging. (III) The results of the imaging corresponding to the light intensity related threshold. The sampling time of the three methods is controlled to be the same. There are all 2500 samplings.

around 10^{-2}. In this case, the estimation error has a very small influence on the imaging results. Therefore, there is no significant difference in the imaging effects of the three methods. Although our time-adaptive imaging method has not made a breakthrough in performance under the same sampling time, the adopted threshold setting method with equal estimation error greatly simplifies the design difficulty of the control circuit.

4. Conclusion

In this paper, a time-adaptive sampling method is proposed, and a sampling time adaptive single photon compressive imaging system is built. The theory of threshold of light intensity estimation accuracy is deduced, and then a FPGA-based sampling control module is developed. Finally, the experiment results show that our proposed imaging method can automatically adjust sampling time according to different light intensities. Moreover, compared to the existing time-fixed imaging, the performance of the proposed time-adaptive imaging has no degradation under the same sampling time condition. Although our proposed method has not achieved a breakthrough in performance, the adopted threshold setting method with equal estimation error greatly simplifies the design difficulty of the control circuit.

References

[1] H. M. Qu, Y. F. Zhang, Z. J. Ji, and Q. Chen, "The performance of photon counting imaging with a Geiger mode silicon avalanche photodiode," *Laser Phys. Lett.*, vol. 10, pp. 315–324, 2013.
[2] X. F. Liu, X. R. Yao, C. Wang, X. Y. Guo, and G. J. Zhai, "Quantum limit of photon-counting imaging based on compressed sensing," *Opt. Exp.*, vol. 25, no. 4, pp. 3286–3296, 2017.
[3] B. Sun *et al.*, "3D computational imaging with single-pixel detectors," *Science*, vol. 340, no. 6134, pp. 844–847, 2013.
[4] G. A. Howland, J. C. Howell, and P. B. Dixon, "Photon-counting compressive sensing laser radar for 3D imaging," *Appl. Opt.*, vol. 50, no. 31, pp. 5917–5920, 2011.
[5] M. F. Duarte *et al.*, "Single-pixel imaging via compressive sampling," *IEEE Signal Process. Mag.*, vol. 25, no. 2, pp. 83–91, Mar. 2008.
[6] W. Song, D. Weng, L. Yue, Y. Wang, and Y. Zheng, "Three-dimensional reconstruction for photon counting imaging using a planar catadioptric method," in *Proc. Conf. Lasers Electro-Opt. Pac. Rim*, 2017.
[7] W. K. Yu, X. R. Yao, X. F. Liu, G. J. Zhai, and Q. Zhao, "Compressed sensing for ultra-weak light counting imaging," *Opt. Precis. Eng.*, vol. 20, no. 10, pp. 2283–2292, 2012.

[8] K. M. Du *et al.*, "Photon-counting imaging system based on compressive sensing," *Inf. Laser Eng.*, vol. 41, no. 2, pp. 363–368, 2012.
[9] V. Studer, J. Bobin, M. Chahid, H. S. Mousavi, E. Candes, and M. Dahan, "Compressive fluorescence microscopy for biological and hyperspectral imaging," *Proc. Nat. Acad. Sci. USA.*, vol. 109, no. 26, pp. 10136–10137, 2012.
[10] R. M. Willett, M. F. Duarte, M. A. Davenport, and R. G. Baraniuk, "Sparsity and structure in hyperspectral imaging: Sensing, reconstruction, and target detection," *IEEE Signal Process. Mag.*, vol. 31, no. 1, pp. 116–126, Jan. 2014.
[11] X. Shi, H. Li, Y. Bai, and X. Fu, "Negative influence of detector noise on ghost imaging based on the photon counting technique at low light levels," *Appl. Opt.*, vol. 56, no. 1, pp. 7320–7326, 2017.
[12] K. Zang *et al.*, "Silicon single-photon avalanche diodes with nano-structured light trapping," *Nature Commun.*, vol. 8, no. 1, 2017, Art. no. 628.
[13] P. A. Morris, R. S. Aspden, J. E. Bell, R. W. Boyd, and M. J. Padgett, "Imaging with a small number of photons," *Nature Commun.*, vol. 6, 2015, Art. no. 5913.
[14] F. Cao, G. Zeng, J. Shi, J. Peng, and Y. Yang, "Computational imaging based on time-correlated single-photon-counting technique at low light level," *Appl. Opt.*, vol. 54, no. 31, pp. 9277–9283, 2015.
[15] J. Romberg, "Imaging via compressive sampling," *IEEE Signal Process. Mag.*, vol. 25, no. 2, pp. 14–20, Mar. 2008.
[16] C. M. Watts *et al.*, "Terahertz compressive imaging with metamaterial spatial light modulators," *Nature Photon.*, vol. 8, no. 8, pp. 605–609, 2014.
[17] T. H. Tsai, P. Llull, X. Yuan, L. Carin, and D. J. Brady, "Spectral-temporal compressive imaging," *Opt. Lett.*, vol. 40, no. 17, pp. 4054–4057, 2015.
[18] J. P. Dumas, M. A. Lodhi, W. U. Bajwa, and M. C. Pierce, "Computational imaging with a highly parallel image-plane-coded architecture: Callenges and solutions," *Opt. Exp.*, vol. 24, no. 6, pp. 6145–6155, 2016.
[19] G. A. Howland, D. J. Lum, M. R. Ware, and J. C. Howell, "Photon counting compressive depth mapping.," *Opt. Exp.*, vol. 21, no. 20, pp. 23822–23837, 2013.
[20] J. C. Howell, "Compressive depth map acquisition using a single photon-counting detector: Parametric signal processing meets sparsity," in *Proc. Conf. Comput. Vis. Pattern Recognit.*, 2012, pp. 96–102.
[21] M. J. Sun *et al.*, "Single-pixel three-dimensional imaging with time-based depth resolution," *Nature Commun.*, vol. 7, 2016, Art. no. 12010.
[22] J. Lin, W. J. He, L. Ye, J. Fang, Q. Chen, and G. H. Gu, "Photon-counting adaptive depth imaging strategy," *Acta Opt. Sin.*, vol. 35, no. 10, pp. 86–93, 2015.
[23] F. Soldevila, B. E. Salvador, P. Clemente, E. Tajahuerce, and J. Lancis, "High-resolution adaptive imaging with a single photodiode," *Sci. Rep.*, vol. 5, 2015, Art. no. 14300.
[24] Y. Yan, H. Dai, X. Liu, W. He, Q. Chen, and G. Gu, "Colored adaptive compressed imaging with a single photodiode," *Appl. Opt.*, vol. 55, no. 14, p. 3711–3718, 2016.
[25] D. B. Phillips *et al.*, "Computational imaging with adaptive spatially-variable resolution," in *Proc. Frontiers Opt.*, pp. FTh5C-5, 2016.
[26] D. B. Phillips *et al.*, "Adaptive foveated single-pixel imaging with dynamic supersampling," *Sci. Adv.*, vol. 3, no. 4, 2017, Art. no. e1601782.
[27] S. Dekel, "Adaptive compressed image sensing based on wavelet-trees," preprint, 2008.
[28] A. Averbuch, S. Dekel, and S. Deutsch, "Adaptive compressed image sensing using dictionaries," *Inf. Process. Manage.*, vol. 43, no. 3, pp. 730–739, 2012.
[29] M. Aβmann and M. Bayer, "Compressive adaptive computational ghost imaging," *Sci. Rep.*, vol. 3, 2013, Art. no. 1545.
[30] H. Dai *et al.*, "Adaptive compressed sampling based on extended wavelet trees," *Appl. Opt.*, vol. 53, no. 29, pp. 6619–6628, 2014.
[31] W. K. Yu, M. F. Li, X. R. Yao, X. F. Liu, L. A. Wu, and G. J. Zhai, "Adaptive compressive ghost imaging based on wavelet trees and sparse representation," *Opt. Exp.*, vol. 22, no. 6, pp. 7133–7144, 2014.
[32] F. Rousset, N. Ducros, A. Farina, G. Valentini, C. D'Andrea, and F. Peyrin, "Adaptive basis scan by wavelet prediction for single-pixel imaging," *IEEE Trans. Comput. Imag.*, vol. 3, no. 1, pp. 36–46, Mar. 2017.
[33] F. Rousset, N. Ducros, F. Peyrin, G. Valentini, C. D'Andrea, and A. Farina, "Time-resolved multispectral imaging based on an adaptive single-pixel camera," *Opt. Exp.*, vol. 26, no. 8, pp. 10550–10558, 2017.
[34] A. Kirmani *et al.*, "First-photon imaging," *Science*, vol. 343, no. 6166, pp. 58–61, 2014.
[35] X. Liu, J. Shi and G. Zeng, "First-photon ghost imaging at low light level," in *Proc. Conf. Lasers Electro-Opt.*, 2017, Paper AM4B.6.
[36] X. Liu, J. Shi, X. Wu, and G. Zeng, "Fast first-photon ghost imaging," *Sci. Rep.*, vol. 8, 2018, Art. no. 5012.
[37] S. M. Ross, *Stochastic Processes*. New York, NY, USA: Wiley, 1983.
[38] C. B. Li, "An efficient algorithm for total variation regularization with applications to the single pixel camera and compressive sensing," M.S. thesis, Dept. Comput. Appl. Math., Rice Univ., Houston, TX, USA, 2009.
[39] C. Li, W. Yin, and Y. Zhang, "User's guide for TVAL3: TV minimization by augmented Lagrangian and alternating direction algorithms," Dept. CAAM, Rice Univ., Houston, TX, USA, CAAM Rep. 20. 46-47, 2009.
[40] C. Li, W. Yin, H. Jiang, and Y. Zhang, "An efficient augmented Lagrangian method with applications to total variation minimization," *Comput. Optim. Appl.*, vol. 56, no. 3, pp. 507–530, 2013.